COMPOSITES & POLYCON 2007
American Composites Manufacturers Association
October 17-19, 2007
Tampa, FL USA

Elastic Buckling Behavior Characteristics of GFRP Pipe with Reinforced Ribs

by

Taek Hee Han, Korea University
Sang Yun Han, Korea University
Young Jong Kang, Korea University

Abstract
The elastic buckling strength of a GFRP (Glass Fiber Reinforced Plastic) pipe reinforced with ribs was evaluated. The height and thickness of a rib and the spacing between two adjacent ribs were considered as factors affecting the buckling strength of the pipe. And also, the ratio of the longitudinal stiffness and transverse stiffness was considered as the parameter affecting on the buckling strength because GFRP is orthotropic material. Buckling strengths of various GFRP pipe models with different shapes and stiffness ratio were evaluated by FE analyses and a formula to estimate the elastic buckling strength of a rib-reinforced pipe made of orthotropic material was suggested from the regression with FE analysis results. Analysis results show that a rib-reinforced pipe has superior buckling strength to a general flat pipe and the suggested formula estimates accurate buckling strength of the rib-reinforced pipe.

Introduction
Materials constituting structures have been changed as time and the development of technology. Stone and wood were used to construct structures before and concrete and steel are being widely used to construct structures. Recent days, fiber reinforced plastic (FRP), which is used to construct airplanes or ships, is initiated to civil engineering and enlarges its applications. The application of FRP is wide in most engineering area and it is introduced to a pipe line system due to the simple geometry of a pipe. Because FRP has high strength and light weight, an FRP structure is designed as a thin walled structure and a buckling problem is a matter in this structure.

In Korea, most pipe lines for water and sewerage are made of cast iron, steel, copper, and concrete. These pipes have the problem of corrosion owing to the characteristics of their own materials and that is a reason of scale, crack, and failure of a pipe. In the case of a cast iron pipe, rust, scale, and bacteria may contaminate supplying water and be a reason to reduce the durability of a pipe as shown in Fig. 1. And the subsidence and breakage of a concrete pipe have been widely observed in most pipe line systems as shown in Fig. 2 and Fig. 3.

To maintain the pipe line system from these problems, replacing and retrofitting of pipes are performed and they require high cost. Thus a glass fiber reinforced plastic (GFRP) pipe is initiated to construct an economic pipe line system. A GFRP pipe has high strength and durability and it is free from corrosion. Because a GFRP pipe is a thin walled structure with buckling problems, ribs were attached on the pipe for the enhancement of buckling strength in this study. Parametric study was performed and a buckling strength was suggested for a GFRP pipe with ribs from the results of finite element analyses.

Finite Element Analysis Model
Finite element analyses were performed with ABAQUS and solid elements with twenty nodes were used for modeling GFRP pipes. Different modulus of elasticity was applied to each direction (circumferential and longitudinal) of a GFRP pipe to consider its orthogonal characteristic. Equivalent single layer theory was adopted for the analysis of the orthogonal GFRP pipe and the moduli of elasticity in the circumferential and longitudinal directions were set as 16,265MPa and 11,478MPa, respectively according to the results of material tests.

The geometry of a GFRP pipe with ribs can be defined with its thickness (t), diameter (D), height of rib (h), width of rib (w), and spacing of rib (S). Because the thickness-diameter ratio (t/D) of a GFRP pipe product is constant as 0.02 when its diameter is larger than 500mm in Korea, t/D was set as 0.02 in modeling a GFRP pipe. And h/D, w/D, and S/D were chosen as main parameters to affect on the buckling strength of the GFRP pipe with ribs. Fig. 4 shows the cross section of the GFRP pipe with ribs and its dimensions. The variable ranges were 0.01~0.04 for h/D, 0.02~0.10 for w/D, and 0.1~0.5 for S/D. Uniform loads were applied with normal direction on the outer side of the pipe and boundary conditions were applied to as shown in Fig. 5.

The buckling problem of a circular arch under uniform pressure has been researched by many researchers such as Timoshenko and Gere (1961). To verify the loading and boundary conditions of a FE model, a circular pipe with 1000mm-diameter and 20mm-thickness was analyzed and its result was compared with the results of other researchers. Its modulus of elasticity was 64.5MPa. The buckling strength of a circular arch is given as Eq. 1. The buckling coefficient was suggested as 3.0 by Timoshenko and Gere in 1961, 4.0 by Papangelis and Trahair in 1987, and 2.77 by Rajasekaran and Padmanabhan in 1989. In this study, the buckling coefficient was calculated as 2.99 from FE analysis and it is similar with the coefficient proposed by Timoshenko and Gere.

$$q_{cr} = \frac{kEI}{R^3} \tag{1}$$

where k : buckling coefficient
E : modulus of elasticity
I : moment of inertia
R : radius of an arch or a pipe.

Because the result of finite element analysis is sensitive to the used number of element constituting the analysis model, the convergence check should be performed by the comparison of results from FE analysis and analytical solution for a well known model. A pipe is composed with curved parts. Thus sufficient number of the element should be used for the full description of its behavior. Fig. 6 and Fig. 7 show the results of convergence check in the circumferential direction and longitudinal direction, respectively. As shown in Fig. 6, the buckling strength was converged within the error ratio of 0.1% when the number of element is larger than 16 in the circumferential direction. And as shown in Fig. 7, the buckling strength was converged within the error ratio of 0.1% when the length-diameter ratio of a pipe (L/D) larger than 10 in the longitudinal direction. As L/D increases or the circumferential stiffness-longitudinal stiffness ratio of a pipe increases, the buckled shape is changed from 2-dimensional mode shape to 3-dimensional model shape. 2-dimensional buckled shape of a pipe has constant cross section along the longitudinal direction as shown in Fig. 8 but 3-dimensional buckled shape of a pipe has variable cross section along the longitudinal direction of the pipe as shown in Fig. 9. This 3-dimensional buckled shape results from the difference of the circumferential and longitudinal stiffness. The orthogonal material and attached ribs of the pipe can make the difference stiffness in each direction.

Analysis Results

Finite element analyses were performed with ABAQUS and solid elements with twenty nodes were used for modeling GFRP pipes. Different modulus of elasticity was applied to each direction (circumferential and longitudinal) of a GFRP pipe to consider its orthogonal characteristics. Main parameters were the height, width, and spacing of the rib and buckling analysis were performed for models with various ribs. Thickness-diameter ratio (t/D) was fixed as 0.02. And h/D, w/D, and S/D were changed within the range of 0.01~0.04, 0.02~0.10, and 0.1~0.5, respectively. Because a plate with ribs can be regarded as a flat plate with the equivalent moment of inertia (EMI), the results from FE analysis (FEA) were compared with the analytical results from Eq. 1 with equivalent moment of inertia. When the buckling strength was calculated by Eq. 1, the buckling coefficient was set as 3.0 from Timoshenko and Gere. Table 1 shows the buckling strengths from FE analyses and Eq. 1 with equivalent moment inertia when w/D is 0.02. As shown in Table 1, results from FEA and EMI are similar when h/D is small, but FEA and EMI show different results as h/D increases. As shown in Fig. 10 and Table 1, the buckling strength of a GFRP pipe with ribs increases as h/D increases. This means that increasing the height of a rib enhances the buckling strength when the diameter of a pipe is constant because of increase of moment inertia. But the height of a rib should be limited in a certain range because a rib may be buckled if it is extremely tall.

FE analysis results show the buckling strength increased proportionally to the rib width-pipe diameter ratio (w/D). The increase of rib's width makes the effect of increasing the thickness of pipe and it increases the moment of inertia of the pipe. Fig. 11 and Fig 12 show the bucking strength as the increase of rib width. Table 2 shows the results from FEA and EMI. Buckling strength from FEA is given as the ratio of buckling strength from EMI. FEA and EMI show similar results when w/D is small, but results from FEA shows smaller buckling strength than that of EMI when w/D increases. Because the height of the rib affects on the moment of inertia much more than the width of the rib, the change of rib height make much effect on the buckling strength. Fig. 13 and Fig. 14 show that the increase of S/D makes the buckling strength small. And results from FEA and EMI have little difference.

Fig. 15~Fig. 19 show the buckled shapes of GFRP pipes with ribs. As shown in Fig. 15, generally the buckled shape is 2-dimensional. The amounts of deformations at far end of the pipe and at the middle part of the pipe is different as shown in Fig. 16 and Fig. 17 and these results from the boundary condition of the restrained far end. The entire GFRP pipe shows 2-dimensional buckled shape but locally 3-dimensional buckled shapes are observed between ribs because the different stiffness by stiffened ribs as shown in Fig. 18 and Fig. 19. In Fig. 18, the buckled shape between ribs has a half cycle but if the spacing is larger as shown in Fig. 19, the buckled shape has more than one cycle and the buckling strength decreases. From the results of FEA, the buckled shape has more than one cycle between stiffened ribs when S/D is larger than 0.5.

A GFRP pipe is composed of orthogonal material which its modulus of elasticity in longitudinal and transverse (circumferential) directions is variable as the change of its matrix and glass fiber. As mentioned prior, the significant different stiffness between longitudinal direction and circumferential direction makes a 3-dimensional buckled shape. Thus, the buckling strength of the GFRP pipe was analyzed as the change of modulus of elasticity ratio (longitudinal modulus of elasticity / circumferential modulus of elasticity, E_L / E_C). In this analysis, the circumferential modulus of elasticity (E_C) was fixed and the longitudinal modulus of elasticity (E_L) was changed. The analysis results are summarized at Table 3 and the buckling strength increases as E_L / E_C increases. Actually, the different stiffness in each direction makes lower buckling strength.

With the results from FE analyses, a formula was proposed to calculate the buckling strength of a circular pipe with stiffened ribs made of isotropic material as Eq. (2). And when this pipe is made of orthotropic material, the buckling strength is calculated with Eq. (3). The results from proposed formula have error range within 7.4% when they compared with those of FE analyses. And these formulas can be applied in the range of $0.005<h/R<0.02$, $0.01<w/R<0.05$, and $0.05<S/R<0.25$.

$$q_{cr} = \frac{3EI}{R^3(1-\nu^2)}\left\{\alpha \ln\left(\frac{h}{2R}\right) + \beta\right\}\left(\frac{w}{2R}\right)^{\kappa} \quad (2)$$

$$q_{cr} = \frac{3E_C I}{R^3(1-\nu^2)}\left\{\alpha \ln\left(\frac{h}{2R}\right) + \beta\right\}\left(\frac{w}{2R}\right)^{\kappa}\left(\frac{E_L}{E_C}\right)^{0.035} \quad (3)$$

$$\kappa = \gamma \ln\left(\frac{h}{2R}\right) + \delta \quad (4)$$

$$\alpha = -0.55\frac{S}{2R} \quad (5)$$

$$\beta = -2.8\frac{S}{2R} + 1 \quad (6)$$

$$\gamma = -\frac{S}{10R} + 0.02 \quad (7)$$

$$\delta = -\frac{S}{2R} + 0.1 \quad (8)$$

where

E : modulus of elasticity

E_L : modulus of elasticity in longitudinal direction

E_C : modulus of elasticity in circumferential direction

I : moment of inertia

R : radius of an arch or a pipe.

ν : Poisson's ratio

w : width of rib

h : height of rib

S : spacing of rib

Conclusion

Buckling analyses were performed for GFRP pipes with ribs and the results showed its enhanced buckling strength. By the FE analyses and regression a formula was proposed to calculate the buckling strength of a pipe with ribs made of orthogonal material. The proposed formula showed sufficient accuracy but it is complex to use directly in the field. Thus the proposed formula should be simplified with further studies.

Acknowledgement

This work was supported by Construction Division of SAMSUNG Corporation.

References

Dutta PK, Hui D. (1997) Creep study of FRP composite rebars for concrete, Proceedings of ICCM-11, Gold Coast, Au.

Papangelis, J.P., Trahair, N.S. (1987) Flexural-Torsional Buckling of Arches, Journal of Structural Engineerings, ASCE, Vol. 113(4), pp.889-906.

Marston (1930) The Theory of External Loads on Closed Conduits, Bulletin No.96, Iowa ENG.,

Timoshenko, S.P., Gere, M. (1961) Theory of Elastic Stability, 2nd Ed., McGraw-Hill, Inc.,

Rajasekaran, S., Padmanabhan, S. (1989) Equations of Curved Beams, Journal of Engineering Mechanics, ASCE, Vol. 115(5), pp.1094-1111.

Simitses GJ., Shaw D, Sheinman I. (1985) Stability of imperfect laminated cylinders: a comparison between theory and experiment, AIAA Journal, Vol. 23, pp.1086-1092.

Spangler (1948) Underground Conduits Transaction ASCE, Vol. 113

Tennyson RC. (1975) Buckling of Laminated Composite Cylinders, Composites, pp.17-24.

Watkins (1993) Structural Mechanics of Buried Pipes, Utah UNI., UT 84322,

Figure – 1. Corrosion in a cast Iron Pipe

Figure – 2. Subsidence of a Concrete Pipe

Figure – 3. Breakage and Collapse of a Concrete Pipe

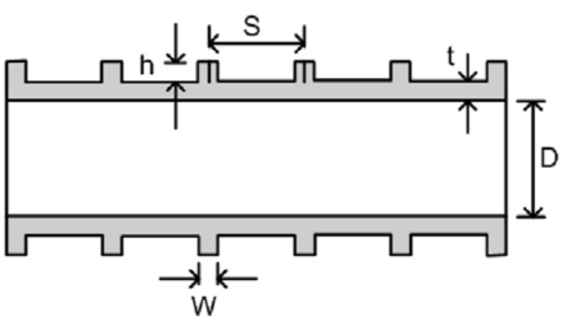

Figure – 4. Cross Section and Dimensions of GFRP Pipe with Ribs

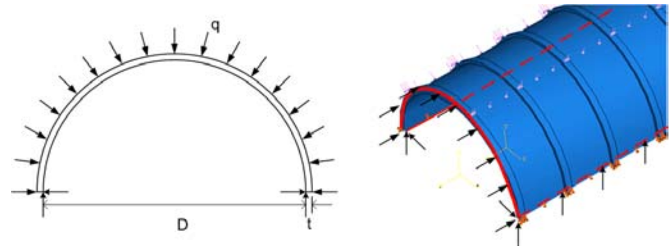

(a) Loading Condition **(b) Boundary Condition**

Figure – 5. Loading and Boundary Conditions

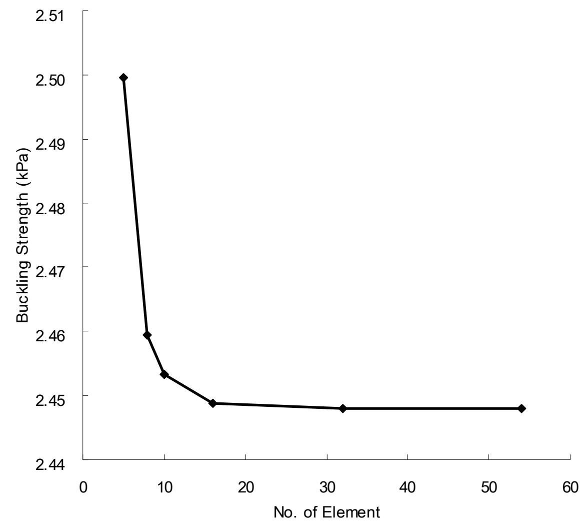

Figure – 6. Convergence in Circumferential Direction

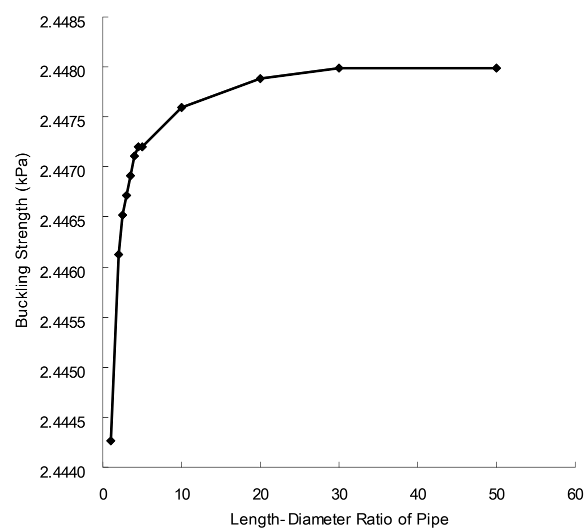

Figure – 7. Convergence in Longitudinal Direction

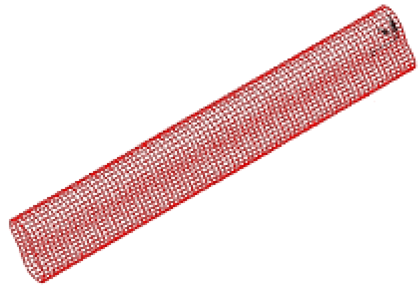

Figure – 8. Two-Dimensional Buckled Shape of Pipe

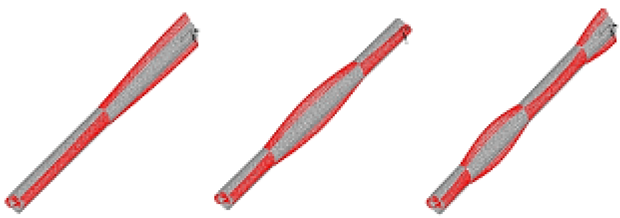

Figure – 9. Three-Dimensional Buckled Shape of Pipe

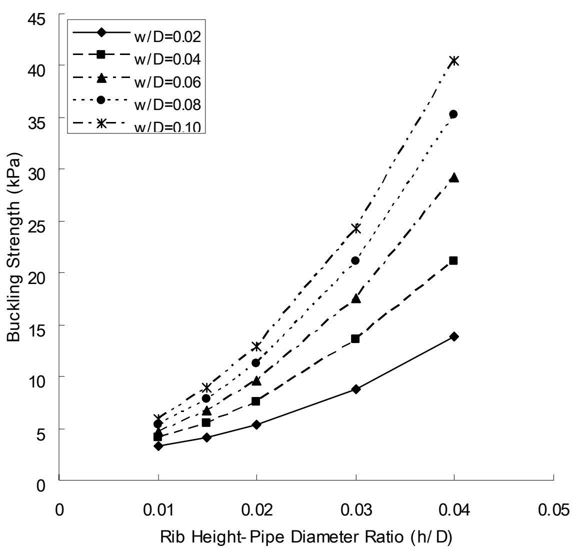

Figure – 10. Buckling Strength-h/D relation (S/D=0.2)

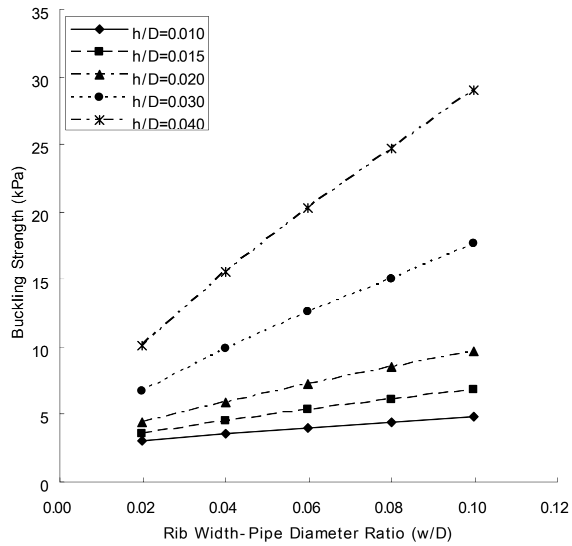

Figure – 11. Buckling Strength-w/D relation (S/D=0.3)

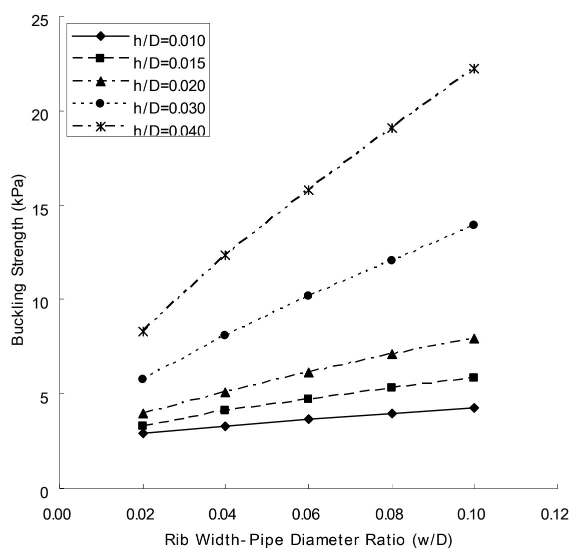

Figure – 12. Buckling Strength-w/D relation (S/D=0.4)

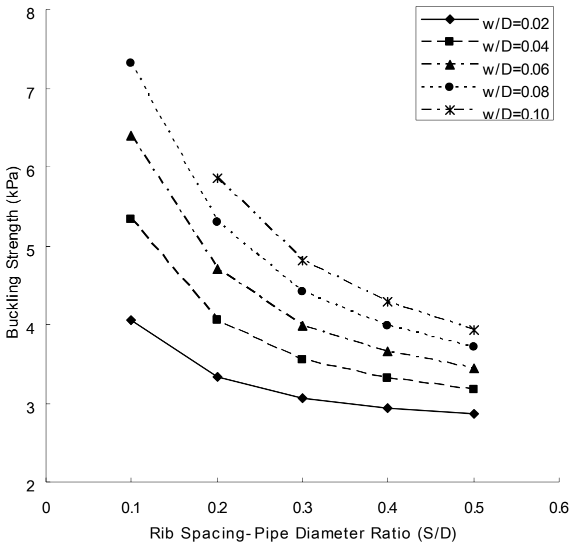

Figure – 13. Buckling Strength-S/D relation (h/D=0.01)

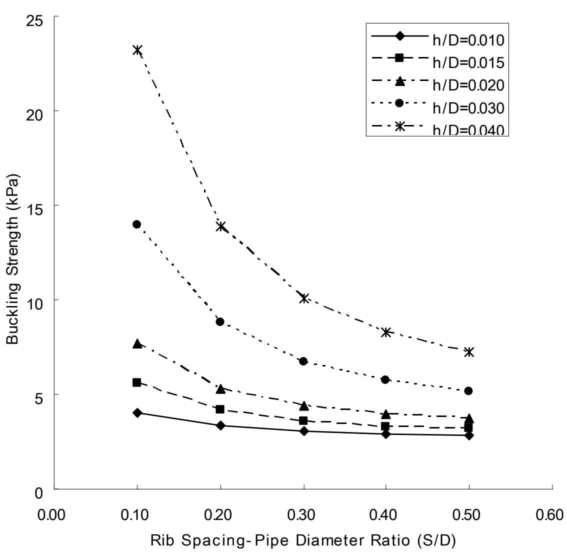

Figure – 14. Buckling Strength-S/D relation (h/D=0.02)

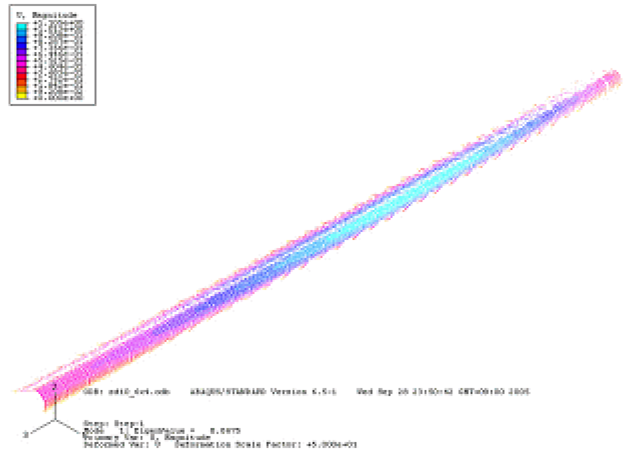

Figure – 15. Buckled Shape of GFRP Pipe with Ribs (w/D=0.06, S/w=10)

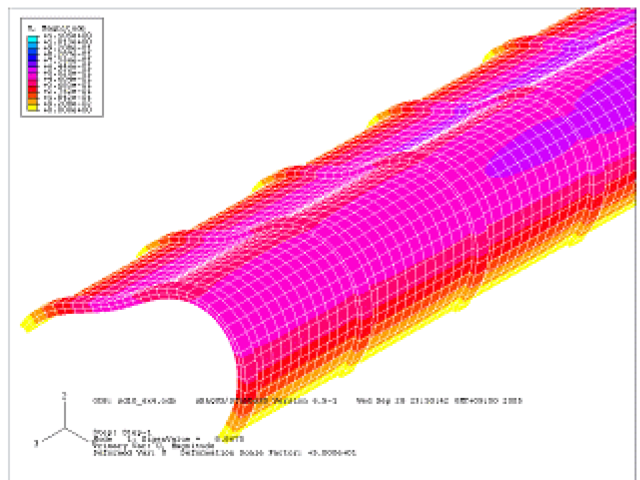

Figure – 16. Buckled Shape at Far End of GFRP Pipe

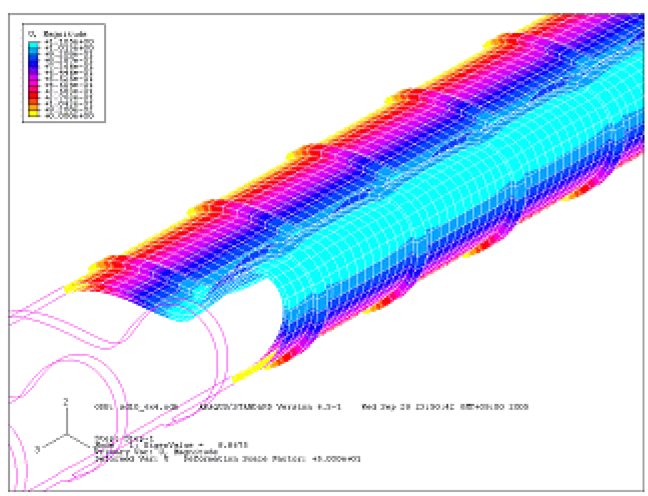

Figure – 17. Buckled Shape at Middle Part of GFRP Pipe

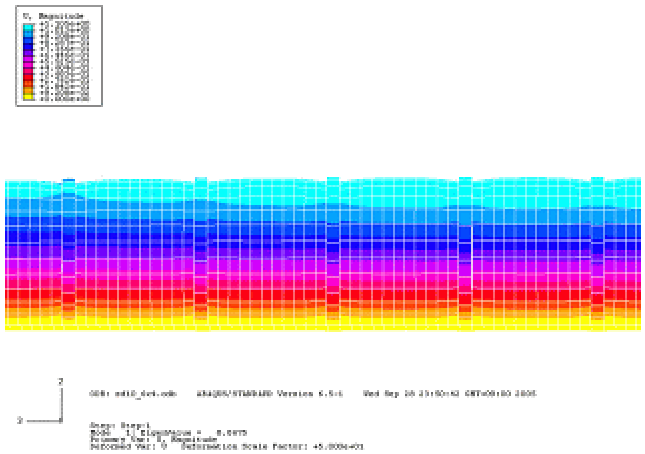

Figure – 18. Buckled Shape between Stiffened Ribs (w/D=0.06, S/w=10)

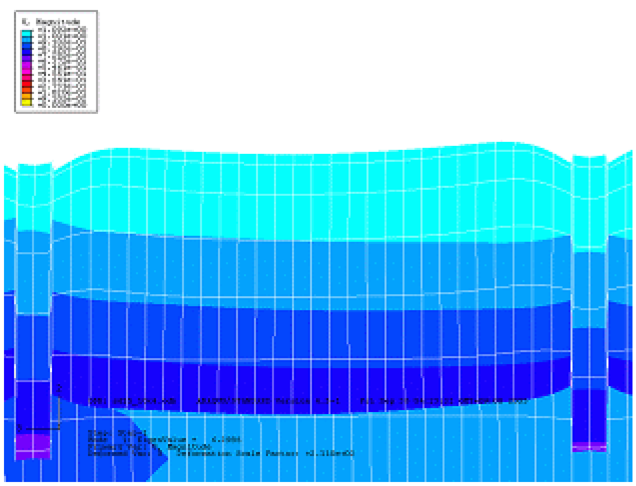

Figure – 19. Buckled Shape between Stiffened Ribs (w/D=0.06, S/w=15)

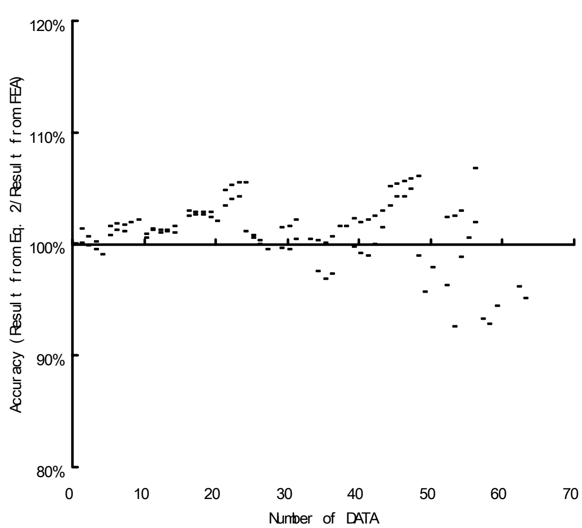

Figure – 20. Accuracy of the Proposed Formula

Table – 1. Buckling Strength of GFRP Pipe with Ribs when w/D=0.02 (kPa)

h/D	Analysis Method	Spacing of Rib-Diameter Ratio (S/D)				
		0.1	0.2	0.3	0.4	0.5
0.010	FEA	4.051	3.327	3.056	2.937	2.860
	EMI	4.011	3.266	3.001	2.866	2.784
0.015	FEA	5.581	4.155	3.615	3.288	3.218
	EMI	5.588	4.120	3.588	3.313	3.144
0.020	FEA	7.703	5.314	4.396	3.976	3.714
	EMI	7.833	5.363	4.447	3.969	3.676
0.030	FEA	13.957	8.807	6.698	5.741	5.155
	EMI	14.692	9.261	7.171	6.064	5.376
0.040	FEA	23.187	13.891	10.057	8.288	7.219
	EMI	25.248	15.421	11.529	9.435	8.127

Table – 2. Buckling Strength Ratio (FEM/EMI)

S/D	w/D	h/D				
		0.01	0.015	0.02	0.03	0.04
0.1	0.02	1.01	0.999	0.983	0.95	0.918
	0.04	1.001	0.986	0.97	0.939	
	0.06	0.993	0.978	0.962	0.932	
	0.08	0.987				
	0.10					
0.2	0.02	1.019	1.008	0.991	0.951	0.901
	0.04	1.009	0.991	0.97	0.923	0.838
	0.06	1.001	0.98	0.959	0.919	0.881
	0.08	0.996	0.976	0.957	0.921	0.888
	0.10	0.992	0.974	0.956	0.924	0.893
0.3	0.02	1.018	1.008	0.989	0.934	0.872
	0.04	1.006	0.98	0.948	0.88	0.817
	0.06	0.994	0.96	0.924	0.858	0.802
	0.08	0.985	0.95	0.916	0.848	0.807
	0.10	0.979	0.944	0.913	0.861	0.819
0.4	0.02	1.025	0.993	1.002	0.947	0.878
	0.04	1.015	0.99	0.955	0.875	0.799
	0.06	1.002	0.965	0.922	0.837	0.765
	0.08	0.991	0.949	0.903	0.821	0.755
	0.10	0.982	0.936	0.892	0.816	0.756
0.5	0.02	1.027	1.023	1.01	0.959	0.888
	0.04	1.02	0.998	0.964	0.88	0.797
	0.06	1.009	0.973	0.928	0.834	0.752
	0.08	0.998	0.954	0.904	0.81	0.612
	0.10	0.98	0.939	0.887	0.796	0.725

Table – 3. Buckling Strength as the Change of Modulus of Elasticity Ratio (kPa)

h/D	w/D	s/D	Modulus of Elasticity Ratio (E_L/E_C)				
			0.2	0.5	0.7	1.0	2.0
0.01	0.10	0.5	3.86	3.91	3.93	3.95	4.02
0.02	0.02	0.2	5.04	5.15	5.19	5.22	5.29
	0.02	0.3	4.27	4.36	4.40	4.43	4.51
	0.02	0.4	3.87	3.95	3.98	4.01	4.08
	0.02	0.5	3.63	3.69	3.71	3.74	3.81
0.03	0.02	0.5	4.94	5.10	5.15	5.21	5.34
	0.04	0.5	6.69	6.96	7.07	7.17	7.40
	0.06	0.5	8.22	8.57	8.71	8.85	9.16
	0.08	0.5	9.69	10.09	10.25	10.41	10.79
	0.10	0.5	11.08	11.53	11.70	11.89	12.32
0.04	0.10	0.5	17.08	17.95	18.30	18.67	19.50

Author(s):

Taek Hee Han :
Korea, Research Professor, Korea University
Doctor of Philosophy - Civil Engineering, Structural Engineering, February 25, 2006.
Master of Science - Civil Engineering, Structural Engineering, February 25, 2001.
Bachelor of Science - Civil Engineering, February 25, 1995.

Young Jong Kang :
Korea, Professor, Korea University
Doctor of Philosophy - Civil Engineering, Structural Engineering, June 10, 1992.
Master of Science - Civil Engineering, Structural Engineering, February 25, 1985.
Bachelor of Science - Civil Engineering, February 25, 1983.

Sang Yun Han :
Korea, Ph. D. Candidate, Korea University
Master of Science - Civil Engineering, Structural Engineering, February 25, 2002.
Bachelor of Science - Civil Engineering, February 25, 2000.